

Multispeed models in off-lattice Boltzmann simulations

André Bardow*

Process & Energy Department, Delft University of Technology, 2628 CA Delft, The Netherlands

Iliya V. Karlin†

*Institute of Energy Technology, Department of Mechanical and Process Engineering, ETH Zurich, 8092 Zurich, Switzerland
and School of Engineering Sciences, University of Southampton, SO17 1BJ Southampton, United Kingdom*

Andrei A. Gusev‡

Institute of Polymers, Department of Materials, ETH Zurich, 8093 Zurich, Switzerland

(Received 26 November 2007; published 28 February 2008)

The lattice Boltzmann method is a highly promising approach to the simulation of complex flows. Here, we realize recently proposed multispeed lattice Boltzmann models [S. Chikatamarla *et al.*, Phys. Rev. Lett. **97** 190601 (2006)] by exploiting the flexibility offered by off-lattice Boltzmann methods. The approach is based on the general characteristic-based algorithm for off-lattice Boltzmann simulations that preserves all appealing properties of the standard lattice Boltzmann method while extending the method to unstructured grids. We show that the use of multispeed models indeed gives rise to major improvements in accuracy. The suggested approach thus renders truly large-scale off-lattice Boltzmann computations practical.

DOI: [10.1103/PhysRevE.77.025701](https://doi.org/10.1103/PhysRevE.77.025701)

PACS number(s): 47.11.-j, 05.20.Dd

The lattice Boltzmann (LB) method has matured into an effective alternative to simulate fluid flow [1]. Based on the Boltzmann equation, the LB method ingeniously couples discretization of velocity and space such that the spatial grid corresponds to the characteristics of the discrete velocity space. A chosen velocity model thus also defines the lattice used for spatial discretization. The LB method then allows for a simple and efficient “stream-and-collide” algorithm to recover hydrodynamics.

Since the coupled discretization is a key step in the LB method, significant research has been invested to find stable and efficient velocity models. Still, only the simplest, low-accuracy LB model (LBM) for isothermal hydrodynamics is fully understood today [2]. This model can be derived from the Boltzmann equation by Gauss-Hermite quadrature in velocity space [3,4]. The discrete velocities are roots of the cubic Hermite polynomial \mathcal{H}_3 .

Higher-order models are desirable, in particular, to achieve complete Galilean invariance in the isothermal simulation [5] and to develop lattice Boltzmann simulations of thermal flows [6]. Recently, it has been demonstrated that higher-order models also allow simulations beyond the Navier-Stokes limit in micro flows [7]. Higher-order Gauss-Hermite quadratures offer a systematic route towards models with larger velocity sets [3]. However, the discrete velocities obtained by this procedure no longer fit into a lattice since the roots of Hermite polynomials of order 4 and higher are irrational. Thus, the standard LB space-time discretization procedure is not applicable for the quadrature-based models. Only recently, a systematic procedure to derive admissible LB velocities has been proposed based on a key relation

between the entropy construction and the roots of Hermite polynomials [2]. The new velocities are then found as rational-number approximations to the (irrational) ratios of the Hermite roots, leading to numerically stable LBMs. Thus, the theory developed in Ref. [2] reconciled the bottom-up and top-down approaches to the construction of LBMs.

In off-lattice Boltzmann methods, the velocity and space discretizations are independent. Much research has been done on these methods to enhance the geometrical flexibility of the LB method [8]. In contrast, the additional freedom gained in velocity space seems to not have been systematically exploited. In particular, off-lattice Boltzmann methods are not limited to rational-number ratios between the velocities. Thus, the exact Hermite models as well as their rational-number approximations can be readily employed in the off-lattice Boltzmann setting. This approach is studied in the present Rapid Communication. We show that multispeed models improve accuracy and that the Hermite model hierarchy allows for systematic gains.

For the multispeed models, we follow the systematic approach presented in [2]. The discrete velocities are obtained from minimization of the entropy function H under the constraints of mass and momentum conservation. For higher-order models, additional moments of the Maxwell-Boltzmann distribution, such as the constitutive equations for the pressure P^{eq} and the energy flux Q^{eq} , are also enforced. Noteworthy, the correct representation of the energy flux leads to Galilean invariance. As this is achieved by the fourth- and higher-order Hermite models, we limit our discussion to the fourth- and fifth-order cases.

For these models, the following equilibrium populations f_i^{eq} are obtained from the minimization using a series expansion in powers of the mean velocity u around the zero-velocity equilibrium [2]:

*a.bardow@tudelft.nl

†karlin@lav.mavt.ethz.ch

‡gusev@mat.ethz.ch

$$f_i^{\text{eq}} = \rho W_i \left\{ 1 + \frac{c_{i\alpha}}{T_0} + \frac{u_\alpha u_\beta}{2T_0^2} (c_{i\alpha} c_{i\beta} - T_0 \delta_{\alpha\beta}) + \frac{u_\alpha u_\beta u_\gamma}{6T_0^3} c_{i\gamma} (c_{i\alpha} c_{i\beta} - 3T_0 \delta_{\alpha\beta}) \right\}. \quad (1)$$

Here, f_i^{eq} is the equilibrium particle velocity distribution function along the i th velocity direction, c_i is the corresponding discrete velocity, T_0 is the reference temperature, and ρ is the density. The subscripts α , β , and γ denote vector components along the different spatial dimensions, and summation is performed over repeated indices.

In the one-dimensional case, the four velocities of the fourth-order model will be denoted $\{\pm m, \pm n\}$ where we assume $m < n$ without loss of generality. The following weights W_i and reference temperature T_0 are obtained [2]:

$$W_{\pm m} = \frac{r^2 - 5 + \sqrt{r^4 - 10r^2 + 1}}{12(r^2 - 1)}, \quad (2)$$

$$W_{\pm n} = \frac{5 - r^2 - \sqrt{r^4 - 10r^2 + 1}}{12(r^2 - 1)}, \quad (3)$$

$$T_0 = n^2 \frac{r^2 + 1 + \sqrt{r^4 - 10r^2 + 1}}{6}, \quad (4)$$

where the ratio between the velocities is defined as $r = m/n$. This velocity ratio $r < 1$ is the remaining degree of freedom used to recover the cubic term in the energy flux Q^{eq} . This is achieved by choosing the velocities equal to the roots of \mathcal{H}_4 —i.e., $m = \sqrt{3 - \sqrt{6}}$ and $n = \sqrt{3 + \sqrt{6}}$, leading to $r_4^* = \sqrt{3} - \sqrt{2}$. The velocity ratio r_4^* is the decisive characteristic for the exact Hermite multispeed model \mathcal{H}_4 .

For the fifth-order model, the five velocities are $\{0, \pm m, \pm n\}$ in one dimensional (1D). Weights and reference temperature are obtained in the same manner, leading to [2]

$$W_0 = \frac{-3 - 3r^4 + 54r^2 - (r^2 + 1)D_5}{75r^2}, \quad (5)$$

$$W_{\pm m} = \frac{9r^4 - 6 - 27r^2 + (3r^2 - 2)D_5}{300r^2(r^2 - 1)}, \quad (6)$$

$$W_{\pm n} = \frac{9 - 6r^4 - 27r^2 + (3 - 2r^2)D_5}{300(1 - r^2)}, \quad (7)$$

$$T_0 = n^2 \frac{3r^2 + 3 + D_5}{30}, \quad (8)$$

with

$$D_5 = \sqrt{9r^4 - 42r^2 + 9}. \quad (9)$$

Setting the velocities equal to the roots of the fifth-order polynomial \mathcal{H}_5 —i.e., $\{0, \pm \sqrt{5 - \sqrt{10}}, \pm \sqrt{5 + \sqrt{10}}\}$ —gives the velocity ratio $r_5^* = \frac{\sqrt{5 - \sqrt{2}}}{\sqrt{3}}$ required to recover the highest-order term in the fourth-order moment of the Maxwell-Boltzmann distribution.

The discrete velocities c_i in the D -dimensional case are obtained as tensor products of D copies of the 1D velocities [2]. The term “multi” refers to the fact that the one-dimensional generating sets contain at least two velocities with nonequal nonzero magnitude. The weights are computed as product of the corresponding 1D weights while the reference temperature T_0 is independent of dimension. The speed of sound of the model is given by $c_s^2 = T_0$.

The exact Hermite multispeed models of order 4 and higher have attractive theoretical properties as they allow for recovering higher-order moments of the Maxwell-Boltzmann distribution leading, e.g., to Galilean invariance [2]. These models do, however, not fit into a lattice as the velocity ratios r_i^* are irrational. The theoretical insight into higher-order velocities models can, however, be immediately exploited in off-lattice Boltzmann simulations. The general characteristic-based algorithm for off-lattice Boltzmann simulations [9] provides the basis of the present development. The scheme is derived from the discrete Boltzmann equation

$$\frac{\partial f_i}{\partial t} + \mathbf{c}_i \cdot \nabla f_i = \Omega_i(f(\mathbf{x}, t)), \quad (10)$$

where $f_i(\mathbf{x}, t)$ is the particle velocity distribution function along the i th velocity direction and $\Omega_i(f(\mathbf{x}, t))$ is the collision operator accounting for the rate of change of f_i due to collisions. By (a) integration over a time step dt along the characteristics using the trapezoidal rule with weighting factor θ , (b) introducing a variable transformation [10] $g_i = f_i - dt\theta\Omega_i(f(\mathbf{x}, t))$ (note that $g_i^{\text{eq}} = f_i^{\text{eq}}$), and (c) introducing a characteristic discretization of the advection step, the following numerical scheme is obtained for stepping from time t_n to t_{n+1} for the Bhatnagar-Gross-Krook (BGK) kernel with $\theta = 1/2$ [9]:

$$g_i^{n+1} = g_i^n - dt \left[c_{i\alpha} \frac{\partial g_i^n}{\partial x_\alpha} + \frac{1}{\lambda} (g_i^n - g_i^{\text{eq},n}) \right] + \frac{dt^2}{2} c_{i\alpha} \frac{\partial}{\partial x_\alpha} \left[c_{i\beta} \frac{\partial g_i^n}{\partial x_\beta} + \frac{2}{\lambda} (g_i^n - g_i^{\text{eq},n}) \right] - \frac{dt^3}{2\lambda} c_{i\alpha} \frac{\partial}{\partial x_\alpha} \left[c_{i\beta} \frac{\partial (g_i^n - g_i^{\text{eq},n})}{\partial x_\beta} \right], \quad (11)$$

where the modified relaxation time is given by $\lambda = \tau + dt/2$. The BGK relaxation time τ is related to the viscosity ν of the fluid by $\nu = \tau c_s^2$. While the scheme (11) is fully explicit, the scattering kernel is indeed handled implicitly. Thereby, Eq. (11) allows for time steps larger than the limit $dt < 2\tau$ previously restricting off-lattice methods [9].

A memory-based off-lattice scheme [11] also overcoming the time-step restriction was proposed recently. As the latter approach requires additional memory and computations for a second set of populations, Eq. (11) is used here to implement the multispeed models.

The general characteristic-based off-lattice Boltzmann method (11) leaves entire freedom in the selection of the velocity model independent from spatial and temporal discretization. Here, the standard D2Q9 velocity model [1] is used as a reference case and both the fourth- and fifth-order

Hermite multispeed models are employed in 2D simulations. As the most conservative scenario for comparison, larger time steps are employed in the higher-order models to compensate for the larger velocity sets:

$$\frac{dt_{\mathcal{H}_4}}{dt_{BGK}} = \frac{16}{9}, \quad \frac{dt_{\mathcal{H}_5}}{dt_{BGK}} = \frac{25}{9}. \quad (12)$$

Thereby, the total number of time-stepping operations (=number of populations \times number of time steps) is equal for all schemes. The only difference in the actual computation time is due to a slightly more expensive evaluation of the equilibrium functions (1). As this difference could be removed by the efficient product form for the evaluation of equilibria [12], the computational effort is practically the same for all considered schemes.

The time step (12) is adjusted via a modification of the Mach number $Ma = u/c_s$. To obtain practically incompressible flow, the Mach number is set to $Ma = 0.01$ for the D2Q9 model in all computations. Since the higher-order models should be less sensitive to Mach number, this constraint is slightly relaxed in the multispeed models to allow still for equal Reynolds, Re, and Courant numbers, $Co = |c_i| dt/dx$, in all schemes.

The multispeed models are explored in a numerical case study using the 2D Taylor-Green vortex flow. Since this flow has periodic boundary conditions, the core properties of the schemes can readily be examined independently from boundary condition issues to be discussed elsewhere. The Taylor-Green vortex flow in a box has the analytical solution

$$\begin{aligned} u &= -u_0 \cos(k_1 x) \sin(k_2 y) \exp[-\nu(k_1^2 + k_2^2)t], \\ v &= u_0 \frac{k_1}{k_2} \sin(k_1 x) \cos(k_2 y) \exp[-\nu(k_1^2 + k_2^2)t], \\ p &= p_0 - \frac{u_0^2}{4} \left[\cos(2k_1 x) + \frac{k_1^2}{k_2^2} \cos(2k_2 y) \right] \\ &\quad \times \exp[-2\nu(k_1^2 + k_2^2)t]. \end{aligned} \quad (13)$$

Pressure $p_0 = \rho_0 c_s^2$ is initialized here using $\rho_0 = 1$. Periodic boundary conditions are applied in both directions. Skordos' [13] initial conditions are used. The wave numbers are chosen as $k_1 = 1.0$ and $k_2 = 4.0$. To reflect the different flow variation in the x and y directions, the flow domain $-\pi \leq x, y \leq \pi$ is covered by a regular but nonsquare grid of $N_x \times N_y = 32 \times 128$ elements. Noteworthy, in contrast to standard LB method, the spatial mesh is now no longer coupled to the momentum discretization. Spatial discretization of Eq. (11) is performed by a Galerkin finite-element method using bilinear quadrilateral elements [14]. Since Eq. (11) has been derived from a self-adjoint problem in space, the spatial discretization by the Galerkin method is optimal [15]. The standard diagonal lumping procedure [14] is applied for the mass matrix. The Reynolds number is $Re = 500$. To perform efficient computations, the time steps is chosen as $dt_{BGK} = 50\tau$.

In Fig. 1, the numerical results \mathbf{u}^{num} are compared to the analytical solution \mathbf{u} at $t = 3t_c$. Here, $t_c = \ln 2 / [\nu(k_1^2 + k_2^2)]$ is

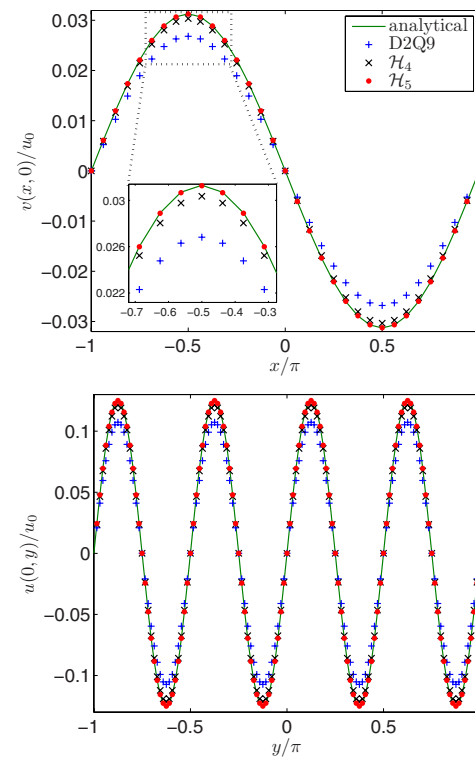


FIG. 1. (Color online) Numerically (symbols) and analytically (solid lines) computed velocity profiles of Taylor-Green vortex flow with $Re = 500$ at $t = 3t_c$ using D2Q9, \mathcal{H}_4 , and \mathcal{H}_5 multispeed models.

the decay half-time of the vortex amplitude. All schemes lead to stable computations. This exemplifies clearly that the time-step restriction commonly associated with off-lattice Boltzmann methods of $dt < 2\tau$ has been successfully overcome.

With respect to the chosen velocity sets, we see a systematic improvement with the employment of higher-order velocity models. The numerical dissipation is lowered—even though larger time steps are employed.

Similar results have been obtained up to $Re = 5000$ with time steps as large as $dt_{BGK} = 500\tau$. In this case, the average of the relative error $\|\mathbf{u}^{num} - \mathbf{u}\|_2 / u_{max}(t)$ where $u_{max}(t) = u_0 \exp[-\nu(k_1^2 + k_2^2)t]$ at the final time $t = 3t_c$ is reduced by factors of 4.1 and 2.1 using the \mathcal{H}_5 model in contrast to the D2Q9 and \mathcal{H}_4 , respectively.

To analyze the improvement beyond the specific discretization method, a simple central finite-difference scheme is also employed for spatial discretization.

Results for the Taylor-Green-vortex flow at Reynolds number $Re = 10^3$ are compared to the finite-element method in Fig. 2. The average of the relative error is shown over time. The time step is $dt_{BGK} = 100\tau$. While the accuracy in time integration is given by the time-stepping scheme and thus is not affected, the significant gain in accuracy by employing higher-order models is also found for finite differences. While the latter gives larger errors in all cases, the gap to the finite-element method can be reduced by using a higher-order model.

The case studies show a systematic improvement by employing higher-order velocity models. We should note that

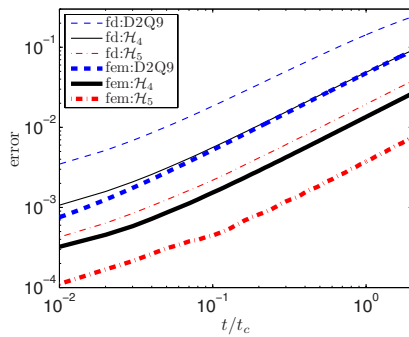


FIG. 2. (Color online) Error over time in Taylor-Green-vortex flow at $\text{Re}=10^3$ using D2Q9, \mathcal{H}_4 , and \mathcal{H}_5 Hermite multispeed models in finite-difference (fd) and finite-element (fem) implementations.

the effect has been minor for low Reynolds numbers where the flow was already fully resolved and the error dominated by other sources. This observation indicates that higher-order models might be particularly suitable for high-Reynolds-number flows previously difficult to realize in off-lattice Boltzmann simulations. As larger velocity sets seem to compensate for coarser grids, the Courant-Friedrichs-Lewy (CFL) limitation may also be lowered.

To analyze the specific choice of Hermite models, the velocity ratio r is systematically varied for the Taylor-Green-vortex flow at $\text{Re}=10^3$. In Fig. 3, the error at $t=2t_c$ is reported. We see a clear convergence with approach to the exact Hermite multispeed model. For both schemes, half of the improvement is only achieved in the last increment towards the exact velocity ratio.

Noteworthy, Fig. 3 mirrors the theoretical analysis in [2] where the monotonicity of the rational-number approximation was studied (Fig. 1 in [2]). The monotonicity analysis showed a steep increase in convergence of the higher-order moments close to the exact solution. The same behavior is now found in solution accuracy.

The theoretical analysis also showed that the convergence to the higher-order moments is conserved by moving from one order to the next [2]. This behavior is also seen in the

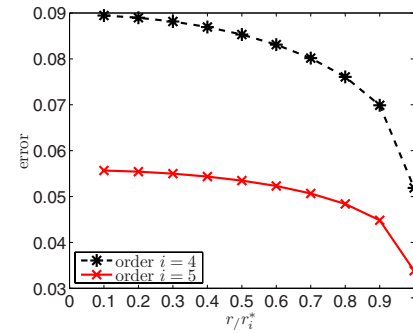


FIG. 3. (Color online) Error at final time $t=2t_c$ as a function of the velocity ratio r_i for orders $i=4,5$.

numerical computations. The error level reached with the exact Hermite model \mathcal{H}_4 corresponds well to the starting level for the five-velocity model. The systematic improvements through the Hermite velocity model hierarchy can therefore be exploited in practical off-lattice computations.

In conclusion, we have realized exact Hermite multispeed models in off-lattice Boltzmann simulations. The computations show that higher-order velocity models lead to major improvements in accuracy. Multispeed models provide a systematic framework where improvements are gained by approaching the optimal velocity ratio given by the irrational Hermite roots and then by increasing the order of the velocity model.

The present paper indicates a clear benefit of off-lattice Boltzmann methods which can readily exploit the advantages of the exact Hermite multispeed models. As the time-step limitation has been overcome, off-lattice Boltzmann methods might challenge the standard LB method. Off-lattice schemes can be further enhanced by incorporating the Boltzmann H theorem [16] or the more efficient higher-order finite elements [17]. The present results indicate that significant gains in accuracy and computational effort for Boltzmann-based simulations can be achieved by exploiting the discretization freedom in time, space, and velocity, giving rise to optimal, problem-adapted methods.

I.V.K. gratefully acknowledges support of CCEM-CH.

- [1] S. Succi, *The Lattice Boltzmann Equation For Fluid Dynamics and Beyond* (Oxford University Press, Oxford, 2001).
- [2] S. S. Chikatamarla and I. V. Karlin, *Phys. Rev. Lett.* **97**, 190601 (2006).
- [3] X. W. Shan and X. Y. He, *Phys. Rev. Lett.* **80**, 65 (1998).
- [4] S. Ansumali, I. V. Karlin, and H. C. Öttinger, *Europhys. Lett.* **63**, 798 (2003).
- [5] Y. H. Quian and S. A. Orszag, *Europhys. Lett.* **21**, 255 (1993).
- [6] P. Lallemand and L. S. Luo, *Phys. Rev. E* **68**, 036706 (2003).
- [7] S. Ansumali, I. V. Karlin, S. Arcidiacono, A. Abbas, and N. I. Prasianakis, *Phys. Rev. Lett.* **98**, 124502 (2007).
- [8] S. Ubertini and S. Succi, *Prog. Comput. Fluid Dyn.* **5**, 85 (2005).
- [9] A. Bardow, I. V. Karlin, and A. A. Gusev, *Europhys. Lett.* **75**, 434 (2006).
- [10] X. He, S. Chen, and G. D. Doolen, *J. Comput. Phys.* **146**, 282 (1998).
- [11] S. Ubertini, G. Bella, and S. Succi, *Math. Comput. Simul.* **72**, 237 (2006).
- [12] S. S. Chikatamarla, S. Ansumali, and I. V. Karlin, *Phys. Rev. Lett.* **97**, 010201 (2006).
- [13] P. A. Skordos, *Phys. Rev. E* **48**, 4823 (1993).
- [14] O. C. Zienkiewicz and R. L. Taylor, *The Finite Element Method* (Butterworth-Heinemann, Oxford, 2000).
- [15] O. C. Zienkiewicz and R. Codina, *Int. J. Numer. Methods Fluids* **20**, 869 (1995).
- [16] I. V. Karlin, A. Ferrante, and H. C. Öttinger, *Europhys. Lett.* **47**, 182 (1999).
- [17] A. Duyster, L. Dernkiewicz, and E. Rank, *Int. J. Numer. Methods Eng.* **67**, 1094 (2006).